Oxidation of CaMKII determines the cardiotoxic effects of aldosterone

Document status and date:
Published: 01/12/2011

DOI:
10.1038/nm.2506

Document Version:
Publisher's PDF, also known as Version of record

Document license:
Taverne

Please check the document version of this publication:

• A submitted manuscript is the version of the article upon submission and before peer-review. There can be important differences between the submitted version and the official published version of record. People interested in the research are advised to contact the author for the final version of the publication, or visit the DOI to the publisher's website.
• The final author version and the galley proof are versions of the publication after peer review.
• The final published version features the final layout of the paper including the volume, issue and page numbers.

Link to publication

Download date: 30 Sep. 2023

Oxidation of CaMKII determines the cardiotoxic effects of aldosterone

B Julie He[1,2], Mei-ling A Joiner[2,12], Madhu V Singh[2,12], Elizabeth D Luczak[2,12], Paari Dominic Swaminathan[2,12], Olha M Koval[2], William Kutschke[2], Chantal Allamargot[3], Jinying Yang[2], Xiaoqun Guan[2], Kathy Zimmerman[4], Isabella M Grumbach[2], Robert M Weiss[2,4], Douglas R Spitz[5], Curt D Sigmund[6], W Matthijs Blankesteijn[7], Stephane Heymans[8–10], Peter J Mohler[11] & Mark E Anderson[1,2]

Excessive activation of the β-adrenergic, angiotensin II (Ang II) and aldosterone signaling pathways promotes mortality after myocardial infarction, and antagonists targeting these pathways are core therapies for treating this condition. Catecholamines and Ang II activate the multifunctional Ca^{2+}/calmodulin-dependent protein kinase II (CaMKII), the inhibition of which prevents isoproterenol-mediated and Ang II–mediated cardiomyopathy. Here we show that aldosterone exerts direct toxic actions on myocardium by oxidative activation of CaMKII, causing cardiac rupture and increased mortality in mice after myocardial infarction. Aldosterone induces CaMKII oxidation by recruiting NADPH oxidase, and this oxidized and activated CaMKII promotes matrix metalloproteinase 9 (MMP9) expression in cardiomyocytes. Myocardial CaMKII inhibition, overexpression of methionine sulfoxide reductase A (an enzyme that reduces oxidized CaMKII) or NADPH oxidase deficiency prevented aldosterone-enhanced cardiac rupture after myocardial infarction. These findings show that oxidized myocardial CaMKII mediates the cardiotoxic effects of aldosterone on the cardiac matrix and establish CaMKII as a nodal signal for the neurohumoral pathways associated with poor outcomes after myocardial infarction.

Myocardial infarction is a common clinical presentation of ischemic heart disease, a leading cause of death worldwide[1]. Excessive neurohumoral activity, including sympathetic stimulation and renin-angiotensin-aldosterone activation, promotes heart failure and sudden death in individuals with myocardial infarction. Myocardial CaMKII is now recognized as a downstream signal that is necessary for the pathological responses to β-adrenergic–receptor agonist[2] and Ang II (ref. 3) stimulation, but the potential intersection between CaMKII and cardiac aldosterone signaling is unexplored. Circulating aldosterone concentrations increase in individuals after myocardial infarction[4], and augmented plasma aldosterone concentrations increase the risk of early mortality after myocardial infarction[5]. Aldosterone activates the mineralocorticoid receptor, and although antagonists of this receptor substantially reduce mortality after myocardial infarction[6,7], the cellular pathways activated by aldosterone that contribute to increased mortality after myocardial infarction are largely unknown. Aldosterone favors renal sodium reabsorption in the distal convoluted tubule[8], but recent evidence suggests that aldosterone has direct effects on the myocardium to increase the amount of reactive oxygen species (ROS)[9,10]. We recently identified a molecular mechanism in which CaMKII is activated during myocardial infarction or by infusion of Ang II by oxidation of paired methionines (Met281 and Met282) in the CaMKII regulatory domain[3]. The apparent association of aldosterone with an increased amount of myocardial ROS and premature death suggests that oxidized CaMKII (ox-CaMKII) could have a key role in the pathological responses to aldosterone signaling in the heart.

Using a mouse myocardial infarction model, we infused aldosterone to approximate the plasma aldosterone concentrations measured in patients with myocardial infarction[11,12]. We found enhanced cardiac rupture in these mice compared to mice with myocardial infarction infused with vehicle, with a corresponding increase in CaMKII activity and upregulation of matrix metalloproteinase 9 (encoded by *Mmp9*). Our findings reveal a previously unidentified role for CaMKII in the aldosterone pathway and highlight a previously unknown ability of myocytes to adversely affect the cardiac matrix after myocardial infarction.

RESULTS

Aldosterone stimulates CaMKII oxidation and activation
Within 15 min after administration, aldosterone stimulated cardiac ROS, as detected by the ROS fluorescent indicator dihydroethidium (DHE),

in wild-type (WT) mice and, to a significantly lesser degree, in $Ncf1^{-/-}$ ($p47^{phox-/-}$) mice, which lack functional NADPH oxidase[13] ($P = 0.003$ by analysis of variance (ANOVA); $P < 0.05$ for $Ncf1^{-/-}$ given aldosterone versus WT given aldosterone; $P < 0.01$ for WT given aldosterone versus WT given vehicle by Bonferroni's multiple comparison test; **Fig. 1a**). To determine whether aldosterone can stimulate CaMKII oxidation, we measured ox-CaMKII levels in hearts from aldosterone- and vehicle-infused mice using an antiserum against oxidized Met281-Met282 in the CaMKII autoregulatory domain[3]. We detected increased ox-CaMKII levels by immunofluorescence (**Fig. 1b**) and by immunoblotting of heart lysates from aldosterone-infused mice compared to vehicle-infused mice ($P = 0.021$; **Supplementary Fig. 1a**), and we confirmed that increased ox-CaMKII levels led to an increase in Ca^{2+}/calmodulin–autonomous CaMKII activity without a change in total CaMKII activity ($P = 0.019$; **Fig. 1c**) in the myocardia of aldosterone-infused mice compared to vehicle-infused mice. We previously showed that Ang II infusion can increase CaMKII oxidation[3,14]. To determine whether aldosterone contributes to the increase in myocardial ox-CaMKII after treatment with Ang II, we infused mice for 6 d with Ang II in the presence or absence of the mineralocorticoid receptor antagonist spironolactone. We found that hearts from mice infused with Ang II and spironolactone had a similar degree of CaMKII oxidation compared to mice that received Ang II and vehicle (**Supplementary Fig. 1b**), suggesting that Ang II can increase ox-CaMKII independently of aldosterone. Alternatively, an increase in Ca^{2+}/calmodulin–autonomous CaMKII activity can result from Thr287 autophosphorylation. We found that the level of cardiac CaMKII Thr287 phosphorylation was similar in vehicle- and aldosterone-infused mice (**Supplementary Fig. 1c**),

consistent with a view that aldosterone increases CaMKII activity preferentially by Met281-Met282 oxidation.

We next used cultured neonatal myocytes to further characterize the mechanism underlying aldosterone-induced ROS and CaMKII oxidation. Neonatal myocytes responded to a low concentration of aldosterone (10^{-9} mol l^{-1}) with increased ROS, as detected by DHE (**Supplementary Fig. 2a,b**), in agreement with the published K_d value of mineralocorticoid receptor for aldosterone[15], suggesting that aldosterone acts through the mineralocorticoid receptor to induce ROS. Furthermore, both ROS and ox-CaMKII levels were reduced by the mineralocorticoid receptor antagonist spironolactone (**Fig. 1d**). These findings support the hypothesis that aldosterone-stimulated ROS production and CaMKII oxidation require the mineralocorticoid receptor and suggest the possibility that some of the clinical benefit to patients with myocardial infarction treated with spironolactone is derived from myocardial CaMKII inhibition.

NADPH oxidase is activated by aldosterone in endothelial cells[16], and NADPH oxidase is an effective source of ROS for oxidizing CaMKII in the myocardium[3]. Because $Ncf1^{-/-}$ mice showed partial protection from aldosterone-stimulated cardiac ROS (**Fig. 1a**), we investigated the potential role of NADPH oxidase in aldosterone-induced CaMKII oxidation. Pretreatment with the NADPH oxidase inhibitor apocynin prevented aldosterone-stimulated ROS and CaMKII oxidation in neonatal myocytes (**Fig. 1d**). Because Rac1 is essential for NADPH oxidase activation by mineralocorticoid receptor in endothelial cells[16], we next examined the potential requirement for Rac1 by infecting neonatal myocytes with an adenovirus expressing a dominant-negative form of the small GTPase Rac1 (N17rac1)[17]. N17rac1 prevented aldosterone-induced ROS generation (**Fig. 1e**),
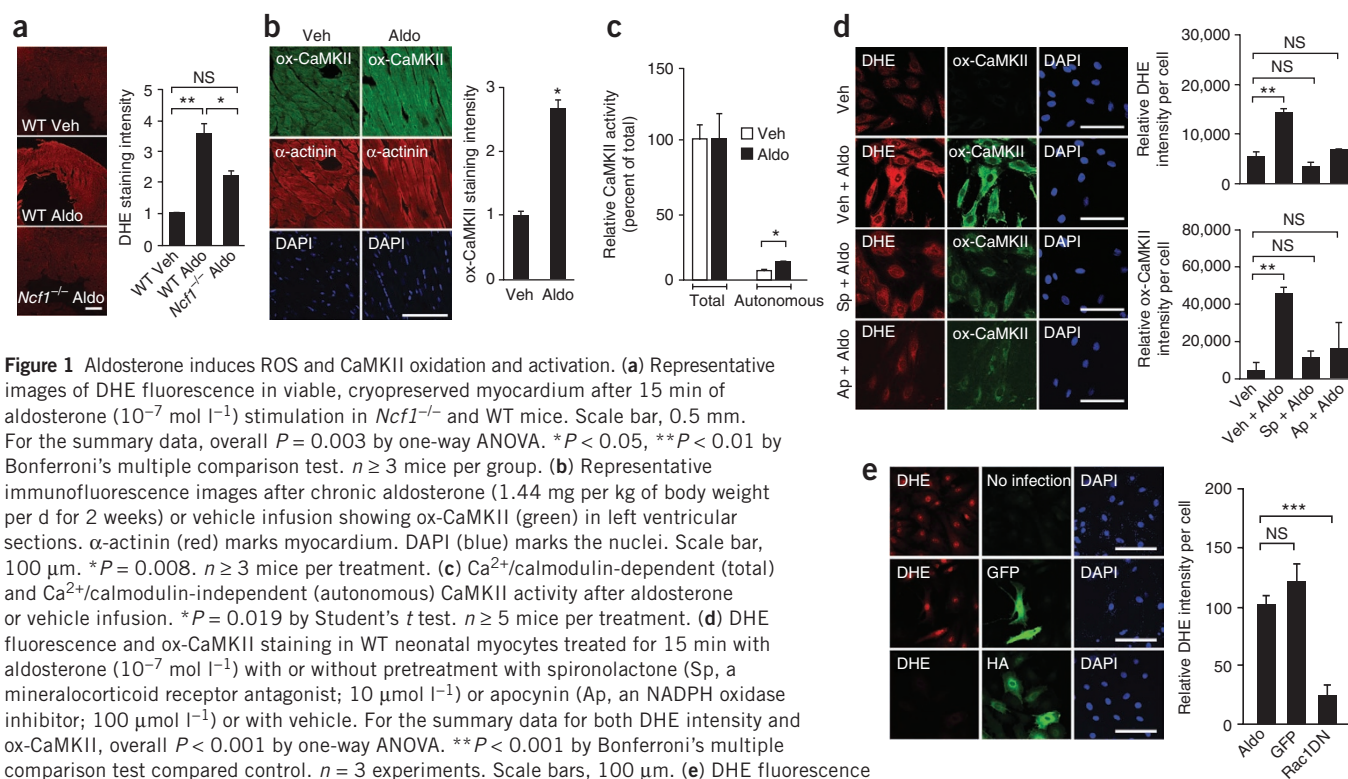

Figure 1 Aldosterone induces ROS and CaMKII oxidation and activation. (**a**) Representative images of DHE fluorescence in viable, cryopreserved myocardium after 15 min of aldosterone (10^{-7} mol l^{-1}) stimulation in $Ncf1^{-/-}$ and WT mice. Scale bar, 0.5 mm. For the summary data, overall $P = 0.003$ by one-way ANOVA. $*P < 0.05$, $**P < 0.01$ by Bonferroni's multiple comparison test. $n \geq 3$ mice per group. (**b**) Representative immunofluorescence images after chronic aldosterone (1.44 mg per kg of body weight per d for 2 weeks) or vehicle infusion showing ox-CaMKII (green) in left ventricular sections. α-actinin (red) marks myocardium. DAPI (blue) marks the nuclei. Scale bar, 100 μm. $*P = 0.008$. $n \geq 3$ mice per treatment. (**c**) Ca^{2+}/calmodulin-dependent (total) and Ca^{2+}/calmodulin-independent (autonomous) CaMKII activity after aldosterone or vehicle infusion. $*P = 0.019$ by Student's t test. $n \geq 5$ mice per treatment. (**d**) DHE fluorescence and ox-CaMKII staining in WT neonatal myocytes treated for 15 min with aldosterone (10^{-7} mol l^{-1}) with or without pretreatment with spironolactone (Sp, a mineralocorticoid receptor antagonist; 10 μmol l^{-1}) or apocynin (Ap, an NADPH oxidase inhibitor; 100 μmol l^{-1}) or with vehicle. For the summary data for both DHE intensity and ox-CaMKII, overall $P < 0.001$ by one-way ANOVA. $**P < 0.001$ by Bonferroni's multiple comparison test compared control. $n = 3$ experiments. Scale bars, 100 μm. (**e**) DHE fluorescence in aldosterone-treated neonatal cardiomyocytes not infected with virus (Aldo) or infected with a hemagglutinin (HA)-tagged dominant negative Rac1 mutant (Rac1DN) or a GFP control construct. $P < 0.001$ between all groups by one-way ANOVA. $***P < 0.001$ by Bonferroni's multiple comparison test for Rac1DN compared to Aldo. $n = 3$ experiments. Scale bars, 100 μm. Aldo, aldosterone; Veh, vehicle; NS, not significant. Data are means ± s.e.m.

Figure 2 Transgenic (TG) myocardial MsrA overexpression reduces CaMKII oxidation. (**a**) Representative immunoblot (IB) of CaMKII oxidation in neonatal myocytes preinfected with an adenoviral (Ad) construct overexpressing Myc-tagged human MsrA or a GFP control construct. For the summary data for $n = 3$ trials, $P = 0.008$ by one-way ANOVA. *$P < 0.05$, **$P < 0.01$ by Bonferroni's multiple comparison test compared to aldosterone-treated, non-infected controls. (**b**) A representative immunoblot shows overexpression of MsrA in hearts from transgenic mice. Myc-tagged human MsrA transgene (arrowhead) has a reduced electrophoretic mobility compared to endogenous MsrA (arrow). (**c**) Cardiac reductase activity is increased in transgenic mice compared to WT littermates. *$P = 0.035$ by Student's t test. $n \geq 3$ mice per genotype. (**d**) A representative immunoblot showing ox-CaMKII and total CaMKII levels in whole-heart homogenates from WT mice infused with aldosterone (1.44 mg per kg of body weight per d for 2 weeks) or vehicle, or from MsrA transgenic mice infused with aldosterone. $n = 6$ mice per group. (**e**) DHE fluorescence of viable, cryopreserved myocardium from WT and MsrA transgenic mice after 15 min of aldosterone (10^{-7} mol l^{-1}) stimulation. Scale bar, 1 mm. $n \geq 3$ mice per genotype. Data are means ± s.e.m.
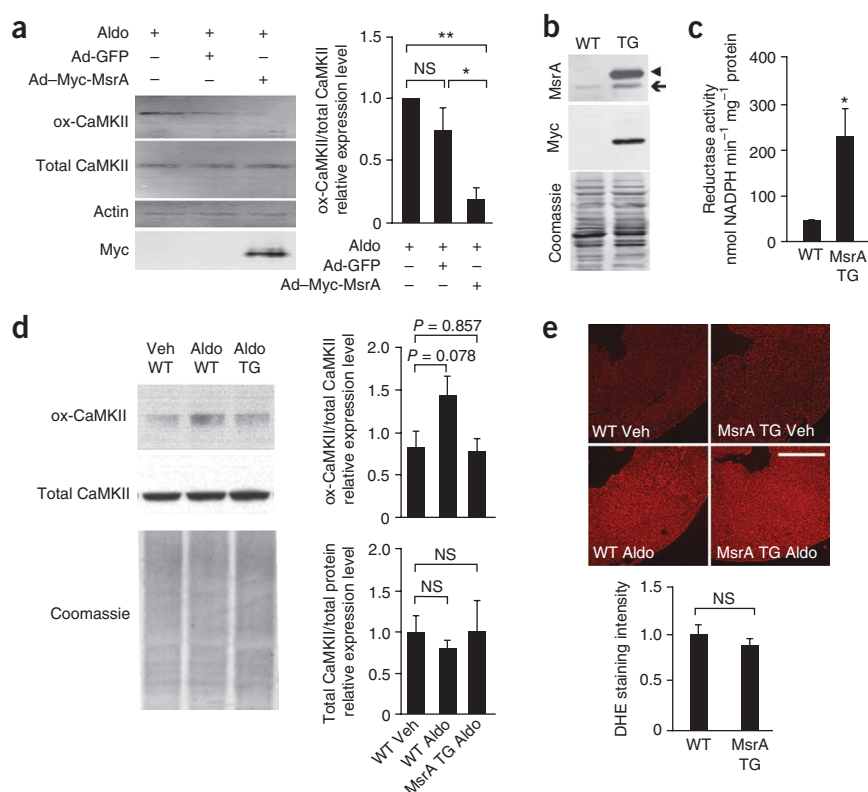
consistent with the hypothesis that mineralocorticoid receptor couples to the NADPH oxidase complex by a Rac1-dependent process in the myocardium. Taken together, these findings suggest that aldosterone increases myocardial ROS levels by mineralocorticoid receptor and Rac1-dependent activation of NADPH oxidase, leading to increased ox-CaMKII levels.

Myocardial MsrA overexpression lowers ox-CaMKII levels

As methionine oxidation is a recently discovered mechanism for CaMKII activation, we sought to better understand the regulation of this dynamic process. Hearts from mice lacking methionine sulfoxide reductase A (MsrA) in all tissues show increased susceptibility to CaMKII oxidation by Ang II and increased mortality after myocardial infarction[3]. To test if myocardial MsrA supplementation could reduce the amount of ox-CaMKII after aldosterone administration, we infected neonatal myocytes with an adenovirus expressing human MsrA. MsrA overexpression reversed aldosterone-stimulated CaMKII oxidation (**Fig. 2a**), suggesting that endogenous concentrations of MsrA in WT myocytes are insufficient for maximal methionine reductase activity against oxidized CaMKII.

We next developed a mouse model of myocardial-restricted MsrA overexpression to determine if CaMKII oxidation is essential to aldosterone-induced pathology *in vivo*. MsrA transgenic mice had increased MsrA protein expression (**Fig. 2b**) and reductase activity (**Fig. 2c**) compared to WT littermates. MsrA transgenic mice had similar baseline left ventricular ejection fractions compared to WT littermates (**Supplementary Fig. 3**). However, the amount of ox-CaMKII was considerably diminished in hearts from MsrA transgenic mice compared to WT littermates in response to aldosterone infusion (**Fig. 2d**). In contrast, and unlike NADPH oxidase deficiency, MsrA overexpression had no effect on aldosterone-induced total ROS production (**Fig. 2e**), as detected by DHE fluorescence, suggesting that MsrA overexpression results in a highly targeted antioxidant effect.

Myocardial infarction and aldosterone promote cardiac rupture

Our data indicate that aldosterone increases the amount of oxidized and activated CaMKII in myocytes *in vivo* and *in vitro*. We next investigated how CaMKII activation could contribute to the cardiotoxic effects of aldosterone after myocardial infarction. After myocardial infarction in humans, plasma aldosterone concentrations may elevate to 20-fold excess over baseline[18] and to as high as 1×10^{-7} mol l^{-1} (ref. 12). We measured plasma aldosterone concentrations in mice after myocardial infarction but found only a modest (approximately twofold) increase, suggesting that robust elevation in circulating aldosterone concentrations after myocardial infarction is not characteristic of mice. To 'humanize' our mouse model, we infused mice with aldosterone to reach a concentration sevenfold over baseline (low dose), similar to that commonly observed in humans with heart failure[19]. In addition, to mimic what is seen in very high risk individuals with severely elevated Aldo after myocardial infarction[11,12], we infused mice with aldosterone to approximate a 20-fold increase in circulating aldosterone concentration over baseline (high dose) (**Supplementary Fig. 4**). WT mice infused with aldosterone and subjected to myocardial infarction (MI+Aldo mice) had significantly reduced survival at the high dose and showed a trend toward reduced survival at the low dose within the first 5 d after surgery, as compared to WT mice infused with vehicle and subjected to myocardial infarction (MI+Veh mice; 34.5% survival with high-dose aldosterone compared to 69.0% survival with vehicle ($P = 0.007$) and 42.9% survival with low-dose aldosterone compared to 69.0% survival with vehicle ($P = 0.083$); **Fig. 3a**). Notably, excess mortality in the MI+Aldo group was a result of cardiac rupture (**Fig. 3b,c**). Because MI+Aldo mice given the high dose of aldosterone had the most prominent rupture and mortality phenotype, we used the high dose in all subsequent studies.
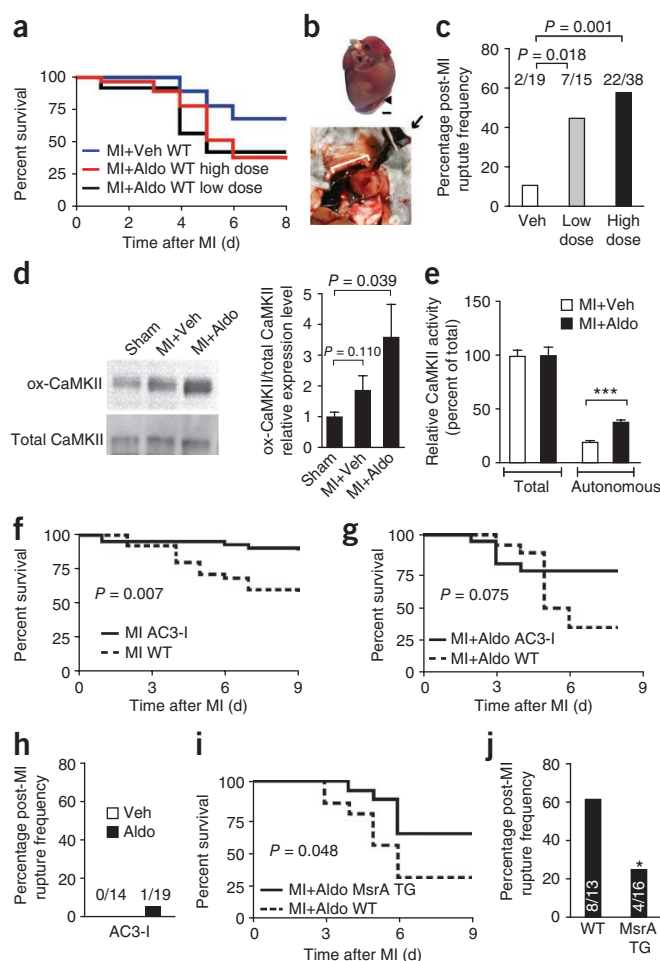
Two weeks after myocardial infarction, we found significantly increased ox-CaMKII levels in cardiac lysates from MI+Aldo mice as

Figure 3 Aldosterone increases mortality after myocardial infarction (MI) by promoting myocardial rupture. (**a**) Kaplan-Meier survival curve for WT mice after MI+Veh, MI+Aldo high-dose or MI+Aldo low-dose treatment. $n \geq 15$ mice per treatment. (**b**) Necropsy of a representative MI+Aldo-treated WT mouse. Forceps (arrow) retract clotted blood from the ruptured heart. The rupture site is indicated with an arrowhead. Scale bar, 1 mm. (**c**) Rupture frequency in WT mice after MI+Veh, MI+Aldo low-dose or MI+Aldo high-dose treatment (**Supplementary Fig. 4**; $P = 0.018$ and $P = 0.001$ for the comparisons shown by χ^2 test). The numbers above the bars are the number of mice that underwent cardiac rupture over the total number of mice. (**d**) Representative immunoblot for ox-CaMKII and total CaMKII in cardiac lysates from mice 2 weeks after sham surgery or after myocardial infarction. Summary data are shown for $n = 6$ mice per treatment group. (**e**) Autonomous and total CaMKII activity in myocardial lysates from WT MI+Aldo and WT MI+Veh mice. ***$P < 0.001$ by Student's t test. $n \geq 5$ mice per treatment. (**f**) Kaplan-Meier survival curve for AC3-I and WT littermate mice after myocardial infarction. $n \geq 30$ mice per genotype; $P = 0.007$. (**g**) Kaplan-Meier survival curve for AC3-I and WT littermate mice after MI+Aldo treatment. $n = 15$–19 mice per genotype; $P = 0.075$. (**h**) Cardiac rupture frequency in AC3-I mice after MI+Aldo or MI+Veh treatment. (**i**) Kaplan-Meier survival curve for MsrA transgenic and WT littermate mice after MI+Aldo treatment. $n = 13$–16 mice per genotype; $P = 0.048$. (**j**) Cardiac rupture frequency in MsrA transgenic and WT littermate mice after MI+Aldo treatment. $n = 13$–16 mice per genotype. *$P = 0.047$. Data are means ± s.e.m.

compared to mice with sham surgery ($P = 0.039$; **Fig. 3d**). Moreover, Ca^{2+}/calmodulin–autonomous CaMKII activity was elevated in cardiac lysates at 1 week after myocardial infarction in MI+Aldo compared to MI+Veh mice ($P < 0.001$; **Fig. 3e**). As aldosterone can increase blood pressure and contribute to heart failure after myocardial infarction by increasing renal sodium reabsorption and intravascular volume[18], we next tested whether an increase in blood pressure could contribute to cardiac rupture in MI+Aldo mice. The blood pressure in WT mice infused with aldosterone for 2 weeks was, however, not significantly different compared to vehicle-infused mice (**Supplementary Fig. 5a–c**), probably because our model did not include increased dietary sodium. To test this hypothesis, we repeated the aldosterone infusion in mice whose drinking water was supplemented with 1% NaCl and 0.75% KCl and found a significant increase in systolic blood pressure ($P = 0.020$; **Supplementary Fig. 5d–f**). Likewise, myocardial infarction itself did not significantly increase blood pressure (**Supplementary Fig. 5g–i**). Echocardiographic measurements, performed at 3–6 d after surgery (the time period during which rupture predominantly occurred) indicated equivalent myocardial function in MI+Aldo and MI+Veh mice, and these measurements were similar between MI+Aldo mice succumbing to cardiac rupture and MI+Aldo mice resisting rupture (**Supplementary Fig. 6**). However, there was a trend toward a decreased ejection fraction in MI+Aldo mice with rupture compared to MI+Aldo mice with no rupture ($P = 0.189$; **Supplementary Fig. 6r**), suggesting that increased contractile force is unlikely to underlie the increased propensity toward cardiac rupture in this model. Thus, excessive death caused by cardiac rupture in MI+Aldo mice was associated with increased levels of ox-CaMKII and autonomous CaMKII activity but was independent of effects on blood pressure and myocardial contraction.

**CaMKII inhibition protects against cardiac rupture**

Myocardial CaMKII inhibition is known to reduce adverse left ventricular remodeling 3 weeks after myocardial infarction[2,3]. However, to our knowledge, the potential of myocardial CaMKII to affect mortality after myocardial infarction is untested. Given the elevated CaMKII activity present in MI+Aldo mice, we hypothesized that CaMKII inhibition might improve survival. Accordingly, we observed

a significant survival advantage in mice with genetic, myocardial-specific CaMKII inhibition (AC3-I mice) compared to WT mice in the first week after myocardial infarction ($P = 0.007$; **Fig. 3f**). In AC3-I mice subjected to the MI+Aldo protocol, we found a trend toward protection from mortality (73.7% survival for MI+Aldo AC3-I mice compared to 33.3% survival for MI+Aldo WT littermates ($P = 0.075$; **Fig. 3g**)). MI+Aldo AC3-I mice had a low incidence of cardiac rupture, similar to that of MI+Veh AC3-I mice (**Fig. 3h**), suggesting that the acute effects of aldosterone in promoting cardiac rupture after myocardial infarction require myocardial CaMKII activity.

To determine the role of ox-CaMKII in survival following MI+Aldo, we repeated the myocardial infarction studies in $Ncf1^{-/-}$ and $MsrA^{-/-}$ mice, as well as in MsrA transgenic mice, which we generated for this study. $Ncf1^{-/-}$ mice were protected from MI+Aldo–induced cardiac rupture (with 0/11 mice in this group having cardiac rupture), supporting the importance of ROS in cardiac rupture after myocardial infarction. $MsrA^{-/-}$ mice showed enhanced myocardial apoptosis, maladaptive left ventricular remodeling and increased mortality after myocardial infarction[3]. We found a pronounced susceptibility to rupture in $MsrA^{-/-}$ MI+Aldo mice (7/10 mice in this group had cardiac rupture), whereas MsrA transgenic MI+Aldo mice had a survival advantage ($P = 0.048$; **Fig. 3i**) and were protected from cardiac rupture compared to MI+Aldo WT littermates ($P = 0.047$; **Fig. 3j**). These studies showed that conditions favoring suppression of myocardial ox-CaMKII dramatically improve survival by reducing cardiac rupture in the first week after myocardial infarction.

Figure 4 MMP9 expression in myocytes is associated with aldosterone and cardiac rupture. (**a**) *Mmp9* mRNA levels in WT and AC3-I mice 3 d after myocardial infarction relative to those in WT sham mice. Overall $P < 0.0001$ by one-way ANOVA; $n \geq 3$ mice per treatment. $**P < 0.01$, $***P < 0.001$ by Bonferroni's multiple comparison test. (**b**) MMP9 immunofluorescence in isolated adult mouse ventricular myocytes 24 h after myocardial infarction in the indicated treatment groups. All images are maximum projections from *z*-stacks obtained using confocal microscopy. Inset, higher magnification view of WT MI+Aldo. Scale bars, 20 μm. For the quantification of immunofluorescence, overall $P < 0.0001$ by one-way ANOVA. $***P < 0.001$ by Bonferroni's multiple comparison test. At least ten cytoplasmic regions of interest, each 32 μm², were selected from $n = 5$–10 cells from $n = 3$ mice per treatment group. (**c**) MMP9 immunofluorescence in human myocardium from subjects with myocardial infarction without rupture (control MI) or with rupture (ruptured MI). Images are the maximum projection of *z*-stacks acquired using confocal microscopy. Brightfield (BF) images show cross-sectional myocardial cells in bundles. Inset is a magnification of the boxed area showing intracellular staining of MMP9. For quantification of MMP9 immunofluorescence, only intracellular staining in cardiomyocytes was measured. MMP9 staining had a more punctate appearance within cardiomyocytes in samples from individuals with MI with rupture compared to MI without rupture. Overall $P < 0.001$ by one-way ANOVA; $n \geq 5$ specimens per group. $***P < 0.001$ by Bonferroni's multiple comparison test. Scale bars, 25 μm. Scale bars for inset, 2.5 μm. ROI, region of interest. Data are means ± s.e.m. AU, arbitrary units.
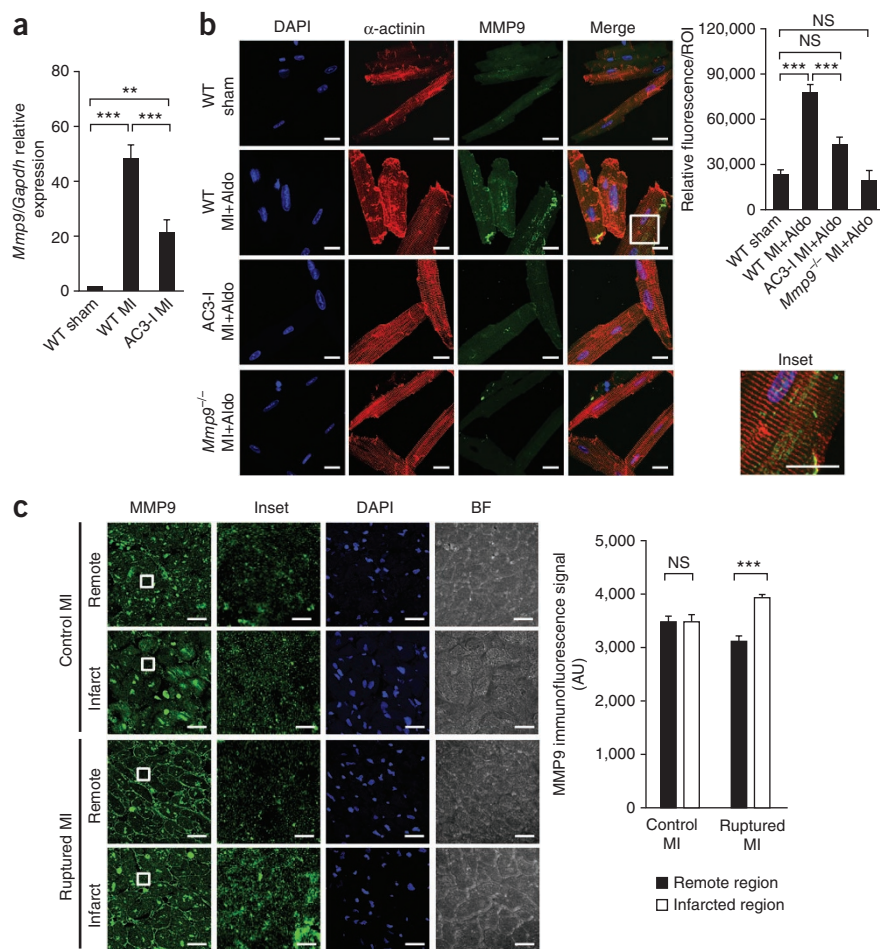
CaMKII increases MMP9 expression

We next focused on the gelatinases MMP2 and MMP9, which are known mediators of the cardiac rupture phenotype in mice[20,21]. We used a gene array comparing mRNA isolated from AC3-I and control hearts after myocardial infarction[22] to identify candidate CaMKII-regulated genes that could contribute to ventricular rupture. These gene array data pointed to a difference in *Mmp9* expression, which we confirmed using quantitative RT-PCR (qRT-PCR): after myocardial infarction, *Mmp9* expression was increased to a significantly lesser degree in AC3-I compared to WT mice (**Fig. 4a**). Neutrophils and macrophages are the predominant sources of MMP9 release after myocardial infarction[21,23]. However, because CaMKII activity is inhibited specifically in cardiomyocytes in AC3-I mice[2], we felt it more likely that the decrease in MMP9 expression occurred in cardiomyocytes. As assessed by immunofluorescence using *z*-stack analysis of images acquired by confocal microscopy, MI+Aldo treatment significantly increased the amount of MMP9 in ventricular cardiomyocytes isolated from the infarcted region in WT but not AC3-I adult mice as compared to cardiomyocytes isolated from adult sham-operated control mice (**Fig. 4b**). *z*-stack analysis further showed that MMP9 expression was cytoplasmic and that MMP9 staining was oriented perpendicularly to that of α-actinin (**Fig. 4b**). These findings suggest that myocardial infarction–provoked cardiac rupture requires a CaMKII–dependent increase in myocardial MMP9 expression.

We repeated the immunofluorescence and *z*-stack analyses on human heart samples obtained from individuals who had died of myocardial infarction with or without rupture. In samples from individuals with rupture, but not in those from individuals without rupture, we found an increase in punctate intracellular staining of MMP9 in cardiomyocytes located in the infarcted region compared to those located in the remote region (**Fig. 4c**). Thus, our findings reveal a parallel increase in cardiomyocyte-derived MMP9 in mice and humans that correlates with cardiac rupture.

Given the contribution of infiltrating immune cells to MMP9 release[21,23], we next assessed whether myocardial CaMKII inhibition might have effects on the cellular response to myocardial infarction. We analyzed myeloperoxidase (MPO), a marker of neutrophil content[24], and found that both MPO immunohistochemical staining (**Fig. 5a**) and MPO activity (**Fig. 5b**) increased after myocardial infarction but were similar in WT and AC3-I mice 24 h after MI+Aldo treatment. The number of MPO-positive cells was also similar in samples from WT MI+Aldo mice with and without cardiac rupture (**Fig. 5a**). We also stained for Mac-3, a macrophage marker, as macrophages are the predominant cell type in the delayed inflammatory influx that follows neutrophil accumulation[21]. In samples 3 d after MI+Aldo treatment, we found no difference in the level of Mac-3 staining between WT and AC3-I mice (**Fig. 5c**). We next asked if the protection from cardiac rupture in AC3-I compared to WT mice after MI+Aldo treatment was due to reduced MMP9 expression in infiltrating inflammatory cells. We performed double immunostaining for the neutrophil membrane marker NIMP-R14 (ref. 25) and MMP9 and for Mac-3 and MMP9 in hearts from WT MI+Aldo and AC3-I MI+Aldo mice. We found no significant
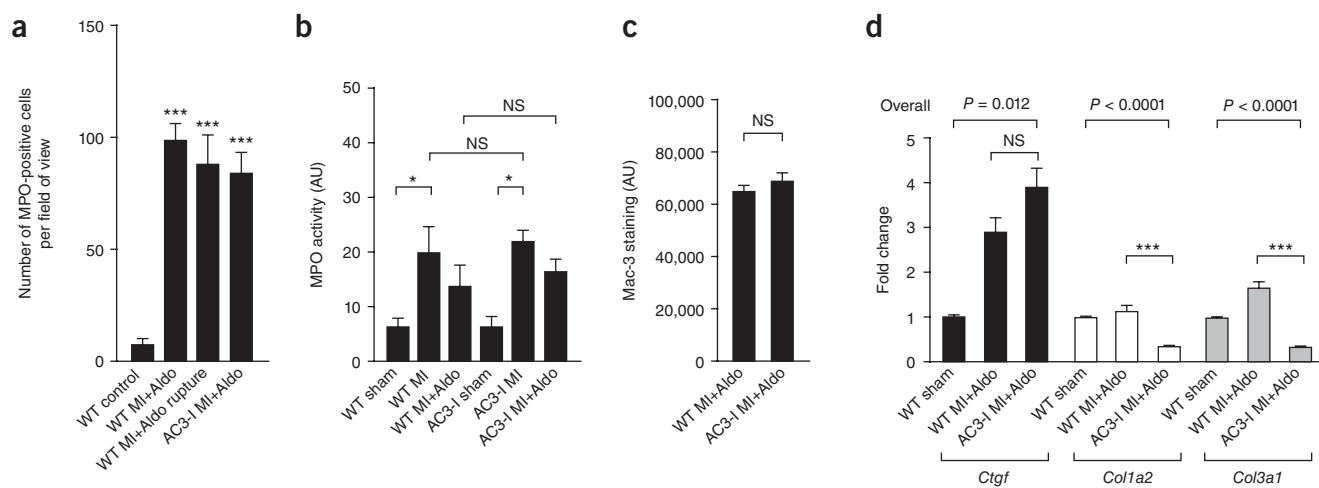
Figure 5 Characterization of the inflammatory and fibrotic responses in AC3-I and WT mice after MI+Aldo treatment. (**a**) Quantification of the number of MPO-positive cells identified by immunohistochemistry in heart tissue sections from control sham-operated WT mice, WT and AC3-I mice 24 h after MI+Aldo treatment, and WT MI+Aldo mice with cardiac rupture. Overall $P < 0.001$ by one-way ANOVA; $n \geq 3$ mice per group. ***$P < 0.001$ by Bonferroni's multiple comparison test compared to WT Control. (**b**) MPO activity in WT and AC3-I mice treated with sham surgery, MI or MI+Aldo as indicated. Overall $P = 0.001$ by one-way ANOVA; $n \geq 3$ mice per group. *$P < 0.05$ by Bonferroni's multiple comparison test. (**c**) Mac-3 staining in WT and AC3-I mice 3 d after MI+Aldo treatment. $n \geq 3$ mice per group. (**d**) Differential regulation of profibrotic genes in WT and AC3-I mice treated with sham surgery or MI+Aldo as indicated. *Ctgf*, the gene encoding connective tissue growth factor; *Col1a2*, the gene encoding collagen type I alpha 2; *Col3a1*, the gene encoding collagen type III alpha 1. $n \geq 4$ mice per group; the indicated overall P values were determined by one-way ANOVA for each bracketed group. ***$P < 0.001$ by Bonferroni's multiple comparison test. (**e**) Masson's trichrome staining showed a similar increase in fibrosis after MI+Aldo treatment in WT and AC3-I mice. P values were determined using a Student's t test; $n \geq 3$ mice per group. Black scale bars, 2 mm; white scale bars, 50 μm. AU, arbitrary units. Data are means ± s.e.m.

differences in MMP9 expression in NIMP-R14 or Mac-3–positive cells between WT and AC3-I mice ($P = 0.787$ and $P = 0.329$, respectively; **Supplementary Fig. 7**), suggesting that inflammatory cells in WT and AC3-I mice produce similar amounts of MMP9. We next assessed cardiac fibrosis after myocardial infarction by examining profibrotic genes known to be activated in cardiomyocytes by a myocyte enhancer factor transcriptional pathway[26]. We found that the levels of *Col1a2* and *Col3a1* mRNA were increased after MI+Aldo treatment of WT mice but were reduced after MI+Aldo treatment of AC3-I mice (**Fig. 5d**). In contrast, *Ctgf* mRNA expression increased equally in WT and AC3-I mice after MI+Aldo treatment. Total collagen deposition, as assessed by Masson's trichrome staining, revealed similar increases in the amount of collagen after MI+Aldo treatment of WT and AC3-I mice (**Fig. 5e**). We interpret these data as indicating that in the setting of myocardial infarction and aldosterone infusion, myocardial CaMKII inhibition suppresses myocardial MMP9 expression without affecting the fibrotic response.

Aldosterone regulates *Mmp9* promoter activity

We next challenged neonatal myocytes with aldosterone and found a significant increase in MMP9 activity by gelatin zymography, whereas MMP2 activity, which is also detectable by this method, was not significantly changed (**Fig. 6a**). We validated *Mmp9* as a transcriptionally

regulated target in neonatal myocytes (**Fig. 6b**), an effect that was attenuated in the presence of the mineralocorticoid receptor antagonist spironolactone (**Supplementary Fig. 2c**). CaMKII activity was crucial for aldosterone-stimulated *Mmp9* expression, as this response was blocked in myocytes which had received pretreatment with an shRNA targeting the major myocardial CaMKII isoform (CaMKIIδ) (**Fig. 6b**). Adenoviral overexpression of CaMKII in neonatal myocytes was sufficient to drive an increase in *Mmp9* expression (**Fig. 6c**). Because *Mmp9*$^{-/-}$ mice are known to resist myocardial infarction–induced cardiac rupture[21], we subjected *Mmp9*$^{-/-}$ mice to MI+Aldo treatment and observed a trend toward protection from rupture (1/8 *Mmp9*$^{-/-}$ mice had rupture compared to 8/13 control C57BL/6 mice ($P = 0.067$)), supporting the concept that MMP9 is needed for increased cardiac rupture in MI+Aldo treated mice.

In astrocytes, CaMKII acts via JNK and c-Jun activation and the subsequent recruitment of the transcription factor AP-1 to the *Mmp9* promoter to induce MMP9 (ref. 27). However, we found no statistical differences between the levels of JNK and c-Jun phosphorylation in cardiac lysates of mice infused with Aldo or vehicle (**Supplementary Fig. 8**), suggesting that AP-1 recruitment is not a major component of aldosterone-induced cardiac signaling activated in these mice. We next analyzed the mouse *Mmp9* gene promoter for potential CaMKII-respon-
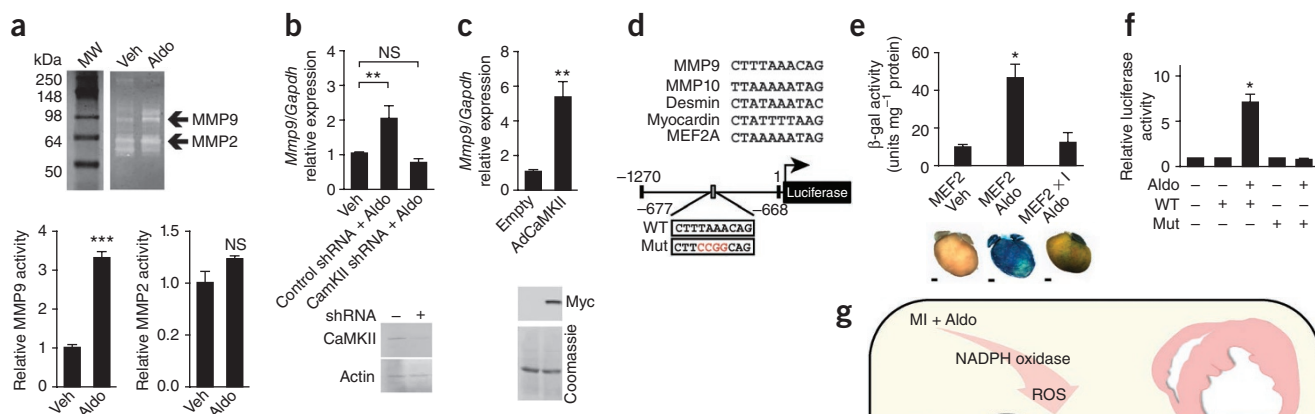
Figure 6 CaMKII promotes cardiac MMP9 expression and activity. (**a**) Representative gelatin zymogram measuring MMP9 and MMP2 activity in the culture supernatant bathing neonatal myocytes treated with vehicle or aldosterone. ***$P < 0.001$. $n = 4$ assays per treatment. (**b**) *Mmp9* mRNA levels measured by qRT-PCR using total RNA isolated from neonatal myocytes 24 h after aldosterone treatment with or without CaMKII knockdown by shRNA. $n = 3$ assays per treatment. Overall $P < 0.001$ by one-way ANOVA. **$P < 0.01$ by Bonferroni's multiple comparison test. The immunoblot verifies CaMKIIδ knockdown. (**c**) *Mmp9* mRNA levels measured by qRT-PCR using total RNA isolated from neonatal myocytes transfected with empty control adenovirus or CaMKII-expressing adenovirus (AdCaMKII). $n = 3$ assays per treatment. **$P = 0.002$. The immunoblot verifies overexpression of Myc-tagged CaMKII. (**d**) Above, alignment of the putative MEF2 binding domain from the mouse *Mmp9* promoter with *bona fide* MEF2 binding domains. Below, schematic diagram of the WT and mutated (Mut) constructs of the *Mmp9* promoter luciferase reporter. (**e**) β-galactosidase expression and activity after aldosterone infusion in *MEF2-lacZ* reporter mice and *MEF2-lacZ* reporter mice interbred with AC3-I mice (MEF2 × I). Scale bars, 1 mm. $n \geq 3$ mice per group; overall $P = 0.002$ by one-way ANOVA. *$P < 0.05$ by Bonferroni's multiple comparison test compared to vehicle. (**f**) *Mmp9*-promoter–driven luciferase activity after aldosterone by the WT and mutant (Mut) constructs, normalized to cotransfected *Renilla* luciferase plasmid. $n = 3$ trials per treatment. Overall $P < 0.001$ by one-way ANOVA. *$P < 0.05$ by Bonferroni's multiple comparison test compared to nontransfected, vehicle-treated control. (**g**) Proposed model for the induction of CaMKII activation by myocardial infarction and aldosterone, leading to myocardial rupture. In the acute setting after myocardial infarction, ox-CaMKII promotes MMP9 upregulation to accelerate matrix breakdown, leading to cardiac rupture and death. MsrA reduces ox-CaMKII levels to prevent MMP9 expression, thereby protecting against cardiac rupture. Data are means ± s.e.m.

sive regulatory sequences and identified an A/T–rich element, similar to other validated binding sites for myocyte enhancer factor 2 (MEF2), located approximately 670 bp upstream of the *Mmp9* transcription start site[28] (**Fig. 6d**). CaMKII is a known upstream activator of MEF2 through phosphorylation-dependent derepression of transcription by type II histone deacytelases[29]. We focused on this candidate MEF2 binding site because aldosterone infusion significantly increased MEF2-driven β-galactosidase activity in the hearts of *MEF2-lacZ* reporter mice[30] compared to vehicle-infused controls (**Fig. 6e**). Aldosterone-induced MEF2 activation was eliminated by interbreeding the *MEF2-lacZ* reporter mice with AC3-I mice (MEF2 × I mice) (**Fig. 6e**), indicating that myocardial CaMKII activity was required for this activation. To determine whether the putative MEF2 binding site was functional, we examined the effects of aldosterone on neonatal myocytes containing intact or mutated versions of an *Mmp9*-promoter–luciferase reporter construct (**Fig. 6d**). Aldosterone treatment significantly increased *Mmp9*-promoter–driven luciferase activity of the intact but not mutated construct (**Fig. 6f**), indicating that the identified region is crucial for aldosterone-mediated transcription of *Mmp9*. *Mmp9* is distinct from canonical MEF2 gene targets, which are involved in muscle differentiation, development and hypertrophy[30,31]. Taken together, our data indicate that cardiomyocyte MMP9 expression is upregulated in the setting of myocardial infarction and aldosterone infusion through a pathway involving CaMKII oxidation and MEF2-dependent transcription (**Fig. 6g**).

DISCUSSION

Our study supports a key role for ROS and myocardial CaMKII in cardiac matrix biology and disease. We show that in the setting of myocardial infarction and high aldosterone levels, CaMKII activation causes mortality due to cardiac rupture with concurrent upregulation of MMP9. Although MMP9 is known to increase cardiac rupture after myocardial infarction, it had previously been presumed that the source of MMP9 was exclusively infiltrating immune cells[21]. Although our results do not rule out the contribution of extramyocardial MMP9 or other proteolytic enzymes (which are likely to also be upregulated in this mouse model) to remodeling after myocardial infarction, they provide evidence for the contribution of cardiomyocyte-delimited CaMKII to a critical threshold of MMP9 activity in the heart. Moreover, although we did not find differences between WT and AC3-I mice in the overall numbers of infiltrating neutrophils or macrophages or in the level of MMP9 expression in these cells, our findings do not exclude the possibility that other functional differences in infiltrating inflammatory cells may contribute to the protective effects of myocardial CaMKII inhibition. Evidence for the active participation of the myocardium in proinflammatory signaling was also provided in another recent study, in which myocardial infarction led to CaMKII-dependent activation of NF-κB–mediated transcription[22]. A previous study found that MEF2-induced *Mmp10* transcription is detrimental to vasculogenesis[32], suggesting that our findings may have far-reaching implications for other processes in which elevated ROS and hyperactive matrix remodeling have key roles in disease progression, such as cancer metastasis[33], atherosclerosis[34] and stroke[35].

Although the role of an ox-CaMKII pathway in the promotion of myocardial MMP9 expression remains unproven in humans, we observed increased myocardial MMP9 levels with rupture after myocardial infarction in mice and humans. Short-term metalloproteinase

inhibition was previously shown to protect against cardiac rupture, but long-term metalloproteinase inhibition led to cardiac dysfunction and premature death as a result of defective neovasculogenesis[21]. These results, combined with previous work from our group and others on the cardioprotective benefits of CaMKII inhibition in structural heart disease[2,14,36,37], suggest that CaMKII inhibition may be a viable alternative to global metalloproteinase inhibition for preventing or reducing the incidence of cardiac rupture and death after myocardial infarction.

Excessive oxidation is a fundamental feature of major cardiovascular diseases and is linked to a wide array of processes associated with maladaptive responses to myocardial infarction, including myocardial hypertrophy[38,39], apoptosis[3], interstitial fibrosis[38,39], increased matrix metalloproteinase activity[39], inflammation[22] and dilation of the left ventricular cavity[3,38]. However, broad spectrum antioxidant supplements have not been beneficial in clinical trials[40–42], although preliminary studies with antioxidants engineered for local action[43] and molecular specificity[44] seem to show benefit. The failure of broad spectrum antioxidant supplements coupled with the preliminary success of molecularly and subcellularly targeted antioxidants suggest that an improved understanding of ROS-responsive disease pathways will be necessary to identify and develop useful new treatments designed to interrupt pathological oxidation processes locally, in the specific signaling pathways most relevant to the progression of cardiovascular disease[45].

Human myocardium after myocardial infarction shows elevated NADPH oxidase activity[46], and hearts from $Ncf1^{-/-}$ mice lacking functional NADPH oxidase are protected from increases in ROS, adverse left ventricular remodeling and death after myocardial infarction surgery[38]. Our results suggest that ROS acts through CaMKII to promote cardiac rupture, as shown, for example, by the protective effects of transgenic overexpression of MsrA.

Neurohumoral pathways initiated by β-adrenergic receptor agonists[47], Ang II (ref. 48) and aldosterone[6,7] are major therapeutically validated targets for reducing mortality and heart failure after myocardial infarction. CaMKII is now recognized to be a downstream signaling protein activated by the β-adrenergic[2] and Ang II (ref. 3) pathways in myocardium, and CaMKII inhibition prevents or attenuates myocardial infarction–induced, isoproterenol-induced and Ang II–induced myocardial hypertrophy, apoptosis and dysfunction[2,3,49]. Here we show that CaMKII is also activated in myocytes by aldosterone through a mineralocorticoid receptor pathway that is not coupled to G-protein receptors, and we also show that CaMKII is required for the early pathological effects of aldosterone after myocardial infarction when both CaMKII activity and ROS levels become elevated. Together with earlier results[2,3], our new findings identify CaMKII as a 'master' signaling node for the neurohumoral pathways targeted by frontline drugs used to treat patients after myocardial infarction.

Cardiac rupture occurs as an early consequence of myocardial infarction and is a particularly challenging clinical problem because it occurs with minimal warning and progresses rapidly to death in the majority of instances despite surgical intervention[50]. Development of preventative therapy is limited by a lack of a molecular understanding of the underlying signaling pathways. The reported incidence of cardiac rupture among myocardial infarction–associated in-hospital deaths can be as high as 15% (ref. 50), similar to the incidence we observed in mice subjected to myocardial infarction without aldosterone treatment. Rupture is the second major cause of cardiac sudden death within the first month after myocardial infarction[51]. Current recommendations support initiation of β-adrenergic–receptor and Ang II antagonist drugs immediately after diagnosis of myocardial infarction[52,53], and our study provides a new mechanistic rationale for a recently initiated clinical study of rapid initiation of mineralocorticoid receptor antagonist drugs to reduce the incidence of mortality after myocardial infarction[54], including mortality caused by ventricular rupture.

METHODS

Methods and any associated references are available in the online version of the paper at http://www.nature.com/naturemedicine/.

Note: Supplementary information is available on the Nature Medicine website.

1. Lopez, A.D., Mathers, C.D., Ezzati, M., Jamison, D.T. & Murray, C.J. Global and regional burden of disease and risk factors, 2001: systematic analysis of population health data. *Lancet* **367**, 1747–1757 (2006).
2. Zhang, R. *et al.* Calmodulin kinase II inhibition protects against structural heart disease. *Nat. Med.* **11**, 409–417 (2005).
3. Erickson, J.R. *et al.* A dynamic pathway for calcium-independent activation of CaMKII by methionine oxidation. *Cell* **133**, 462–474 (2008).
4. Gutierrez-Marcos, F.M. *et al.* Atrial natriuretic peptide in patients with acute myocardial infarction without functional heart failure. *Eur. Heart J.* **12**, 503–507 (1991).
5. Beygui, F. *et al.* High plasma aldosterone levels on admission are associated with death in patients presenting with acute ST-elevation myocardial infarction. *Circulation* **114**, 2604–2610 (2006).

6. Pitt, B. *et al.* Eplerenone, a selective aldosterone blocker, in patients with left ventricular dysfunction after myocardial infarction. *N. Engl. J. Med.* **348**, 1309–1321 (2003).

7. Pitt, B. *et al.* The effect of spironolactone on morbidity and mortality in patients with severe heart failure. Randomized Aldactone Evaluation Study Investigators. *N. Engl. J. Med.* **341**, 709–717 (1999).

8. Reilly, R.F. & Ellison, D.H. Mammalian distal tubule: physiology, pathophysiology, and molecular anatomy. *Physiol. Rev.* **80**, 277–313 (2000).

9. Rude, M.K. *et al.* Aldosterone stimulates matrix metalloproteinases and reactive oxygen species in adult rat ventricular cardiomyocytes. *Hypertension* **46**, 555–561 (2005).

10. Johar, S., Cave, A.C., Narayanapanicker, A., Grieve, D.J. & Shah, A.M. Aldosterone mediates angiotensin II-induced interstitial cardiac fibrosis via a Nox2-containing NADPH oxidase. *FASEB J.* **20**, 1546–1548 (2006).

11. Nakamura, S. *et al.* Possible association of heart failure status with synthetic balance between aldosterone and dehydroepiandrosterone in human heart. *Circulation* **110**, 1787–1793 (2004).

12. Rousseau, M.F. *et al.* Beneficial neurohormonal profile of spironolactone in severe congestive heart failure: results from the RALES neurohormonal substudy. *J. Am. Coll. Cardiol.* **40**, 1596–1601 (2002).

13. Huang, C.K., Zhan, L., Hannigan, M.O., Ai, Y. & Leto, T.L. P47(phox)-deficient NADPH oxidase defect in neutrophils of diabetic mouse strains, C57BL/6J-m *db/db* and *db/+*. *J. Leukoc. Biol.* **67**, 210–215 (2000).

14. Swaminathan, P.D. *et al.* Oxidized CaMKII causes cardiac sinus node dysfunction in mice. *J. Clin. Invest.* **121**, 3277–3288 (2011).

15. Kusch, M., Farman, N. & Edelman, I.S. Binding of aldosterone to cytoplasmic and nuclear receptors of the urinary bladder epithelium of *Bufo marinus*. *Am. J. Physiol.* **235**, C82–C89 (1978).

16. Iwashima, F. *et al.* Aldosterone induces superoxide generation via Rac1 activation in endothelial cells. *Endocrinology* **149**, 1009–1014 (2008).

17. Zimmerman, M.C. *et al.* Requirement for Rac1-dependent NADPH oxidase in the cardiovascular and dipsogenic actions of angiotensin II in the brain. *Circ. Res.* **95**, 532–539 (2004).

18. Weber, K.T. Aldosterone in congestive heart failure. *N. Engl. J. Med.* **345**, 1689–1697 (2001).

19. Swedberg, K., Eneroth, P., Kjekshus, J. & Wilhelmsen, L. Hormones regulating cardiovascular function in patients with severe congestive heart failure and their relation to mortality. CONSENSUS Trial Study Group. *Circulation* **82**, 1730–1736 (1990).

20. Matsumura, S. *et al.* Targeted deletion or pharmacological inhibition of MMP-2 prevents cardiac rupture after myocardial infarction in mice. *J. Clin. Invest.* **115**, 599–609 (2005).

21. Heymans, S. *et al.* Inhibition of plasminogen activators or matrix metalloproteinases prevents cardiac rupture but impairs therapeutic angiogenesis and causes cardiac failure. *Nat. Med.* **5**, 1135–1142 (1999).

22. Singh, M.V. *et al.* Ca2+/calmodulin-dependent kinase II triggers cell membrane injury by inducing complement factor B gene expression in the mouse heart. *J. Clin. Invest.* **119**, 986–996 (2009).

23. van den Borne, S.W. *et al.* Increased matrix metalloproteinase-8 and -9 activity in patients with infarct rupture after myocardial infarction. *Cardiovasc. Pathol.* **18**, 37–43 (2009).

24. Bradley, P.P., Priebat, D.A., Christensen, R.D. & Rothstein, G. Measurement of cutaneous inflammation: estimation of neutrophil content with an enzyme marker. *J. Invest. Dermatol.* **78**, 206–209 (1982).

25. Nahrendorf, M. *et al.* Activatable magnetic resonance imaging agent reports myeloperoxidase activity in healing infarcts and noninvasively detects the antiinflammatory effects of atorvastatin on ischemia-reperfusion injury. *Circulation* **117**, 1153–1160 (2008).

26. Kim, Y. *et al.* The MEF2D transcription factor mediates stress-dependent cardiac remodeling in mice. *J. Clin. Invest.* **118**, 124–132 (2008).

27. Wu, C.Y., Hsieh, H.L., Sun, C.C. & Yang, C.M. IL-1β induces MMP-9 expression via a Ca(2)-dependent CaMKII/JNK/c-JUN cascade in rat brain astrocytes. *Glia* **57**, 1775–1789 (2009).

28. Munaut, C. *et al.* Murine matrix metalloproteinase 9 gene. 5′-upstream region contains *cis*-acting elements for expression in osteoclasts and migrating keratinocytes in transgenic mice. *J. Biol. Chem.* **274**, 5588–5596 (1999).

29. Backs, J., Song, K., Bezprozvannaya, S., Chang, S. & Olson, E.N. CaM kinase II selectively signals to histone deacetylase 4 during cardiomyocyte hypertrophy. *J. Clin. Invest.* **116**, 1853–1864 (2006).

30. Naya, F.J., Wu, C., Richardson, J.A., Overbeek, P. & Olson, E.N. Transcriptional activity of MEF2 during mouse embryogenesis monitored with a MEF2-dependent transgene. *Development* **126**, 2045–2052 (1999).

31. Kolodziejczyk, S.M. *et al.* MEF2 is upregulated during cardiac hypertrophy and is required for normal post-natal growth of the myocardium. *Curr. Biol.* **9**, 1203–1206 (1999).

32. Chang, S. *et al.* Histone deacetylase 7 maintains vascular integrity by repressing matrix metalloproteinase 10. *Cell* **126**, 321–334 (2006).

33. Hiratsuka, S. *et al.* MMP9 induction by vascular endothelial growth factor receptor-1 is involved in lung-specific metastasis. *Cancer Cell* **2**, 289–300 (2002).

34. Timmins, J.M. *et al.* Calcium/calmodulin-dependent protein kinase II links ER stress with Fas and mitochondrial apoptosis pathways. *J. Clin. Invest.* **119**, 2925–2941 (2009).

35. Zhao, B.Q. *et al.* Role of matrix metalloproteinases in delayed cortical responses after stroke. *Nat. Med.* **12**, 441–445 (2006).

36. Khoo, M.S. *et al.* Death, cardiac dysfunction, and arrhythmias are increased by calmodulin kinase II in calcineurin cardiomyopathy. *Circulation* **114**, 1352–1359 (2006).

37. Backs, J. *et al.* The delta isoform of CaM kinase II is required for pathological cardiac hypertrophy and remodeling after pressure overload. *Proc. Natl. Acad. Sci. USA* **106**, 2342–2347 (2009).

38. Doerries, C. *et al.* Critical role of the NAD(P)H oxidase subunit p47phox for left ventricular remodeling/dysfunction and survival after myocardial infarction. *Circ. Res.* **100**, 894–903 (2007).

39. Kinugawa, S. *et al.* Treatment with dimethylthiourea prevents left ventricular remodeling and failure after experimental myocardial infarction in mice: role of oxidative stress. *Circ. Res.* **87**, 392–398 (2000).

40. Yusuf, S., Dagenais, G., Pogue, J., Bosch, J. & Sleight, P. Vitamin E supplementation and cardiovascular events in high-risk patients. The Heart Outcomes Prevention Evaluation Study Investigators. *N. Engl. J. Med.* **342**, 154–160 (2000).

41. Rapola, J.M. *et al.* Randomised trial of alpha-tocopherol and beta-carotene supplements on incidence of major coronary events in men with previous myocardial infarction. *Lancet* **349**, 1715–1720 (1997).

42. Heart Protection Study Collaborative Group. MRC/BHF Heart Protection Study of antioxidant vitamin supplementation in 20,536 high-risk individuals: a randomised placebo-controlled trial. *Lancet* **360**, 23–33 (2002).

43. Jauslin, M.L., Meier, T., Smith, R.A. & Murphy, M.P. Mitochondria-targeted antioxidants protect Friedreich Ataxia fibroblasts from endogenous oxidative stress more effectively than untargeted antioxidants. *FASEB J.* **17**, 1972–1974 (2003).

44. Chen, C.H. *et al.* Activation of aldehyde dehydrogenase-2 reduces ischemic damage to the heart. *Science* **321**, 1493–1495 (2008).

45. Tomaselli, G.F. & Barth, A.S. Sudden cardio arrest: oxidative stress irritates the heart. *Nat. Med.* **16**, 648–649 (2010).

46. Maack, C. *et al.* Oxygen free radical release in human failing myocardium is associated with increased activity of rac1-GTPase and represents a target for statin treatment. *Circulation* **108**, 1567–1574 (2003).

47. Dargie, H.J. Effect of carvedilol on outcome after myocardial infarction in patients with left-ventricular dysfunction: the CAPRICORN randomised trial. *Lancet* **357**, 1385–1390 (2001).

48. Dickstein, K. & Kjekshus, J. & OPTIMAAL Steering Committee of the OPTIMAAL Study Group. Effects of losartan and captopril on mortality and morbidity in high-risk patients after acute myocardial infarction: the OPTIMAAL randomised trial. Optimal Trial in Myocardial Infarction with Angiotensin Antagonist Losartan. *Lancet* **360**, 752–760 (2002).

49. Christensen, M.D. *et al.* Oxidized calmodulin kinase II regulates conduction following myocardial infarction: a computational analysis. *PLOS Comput. Biol.* **5**, e1000583 (2009).

50. Wehrens, X.H. & Doevendans, P.A. Cardiac rupture complicating myocardial infarction. *Int. J. Cardiol.* **95**, 285–292 (2004).

51. Pouleur, A.C. *et al.* Pathogenesis of sudden unexpected death in a clinical trial of patients with myocardial infarction and left ventricular dysfunction, heart failure or both. *Circulation* **122**, 597–602 (2010).

52. Fonarow, G.C., Lukas, M.A., Robertson, M., Colucci, W.S. & Dargie, H.J. Effects of carvedilol early after myocardial infarction: analysis of the first 30 days in Carvedilol Post-Infarct Survival Control in Left Ventricular Dysfunction (CAPRICORN). *Am. Heart J.* **154**, 637–644 (2007).

53. Ambrosioni, E., Borghi, C. & Magnani, B. The effect of the angiotensin-converting-enzyme inhibitor zofenopril on mortality and morbidity after anterior myocardial infarction. The Survival of Myocardial Infarction Long-Term Evaluation (SMILE) Study Investigators. *N. Engl. J. Med.* **332**, 80–85 (1995).

54. Beygui, F. *et al.* Rationale for an early aldosterone blockade in acute myocardial infarction and design of the ALBATROSS trial. *Am. Heart J.* **160**, 642–648 (2010).

ONLINE METHODS

Mouse models. $Ncf1^{-/-}$ ($p47^{phox-/-}$) and $Mmp9^{-/-}$ mice were purchased from the Jackson Laboratory. $MsrA^{-/-}$ mice[3] and $MEF2$-$lacZ$ reporter mice[30] were previously described. We constructed transgenic mice with myocardial expression of the AC3-I peptide, an inhibitor of CaMKII activity, as previously reported[2]. We interbred AC3-I transgenic mice with $MEF2$-$lacZ$ reporter mice for at least five generations. To generate the MsrA transgene, human MsrA cDNA was subcloned into a pBS-αMHC vector backbone (developed by J. Robbins) with flanking MluI and BspEI restriction sites. The transgene was excised, purified and microinjected into pronuclei of B6SJL mice (the progeny of a cross between C57BL/6J and SJL/J mice). Embryonic stem cells from the resulting embryos were derived and ICR blastocysts were microinjected with these cells. Transgenic mice were maintained by backcrossing to C57BL/6J mice for at least four generations. All mice were fed standard mouse chow (7013, Teklad Premier Laboratory Diets) and water *ad libitum*. We performed our studies on 8–20-week-old male mice. We confirmed all genotypes by PCR. All animal procedures met the guidelines set forth by the Institutional Animal Care and Use Committee at the University of Iowa.

Myocardial infarction and echocardiography. Mice underwent myocardial infarction and simultaneous implantation of aldosterone (at a high dose of 1.44 mg per kg of body weight per d or at a low dose of 0.12 mg per kg of body weight per d) or vehicle (5% ethanol in normal saline) containing osmotic minipumps (Model 2002, Alzet) as previously described[3]. Cardiac rupture was identified by blood clotting in the chest cavity and ventricular wall tearing. We recorded the baseline and post-operative transthoracic echocardiograms in conscious mice as previously described[55]. Images were acquired and analyzed by an operator blinded to mouse genotype and treatment.

Cell culture and viral constructs. We isolated adult ventricular myocytes as previously described[56] with minor modifications. Briefly, after Langendorff perfusion, hearts were transferred to a dissecting microscope. We identified the infarcted region by the blanched appearance of a thinned area in the ventricular free wall. The 1–2-mm border zone between this area and myocardium that appeared normal was excised and minced. Neonatal mouse ventricular myocytes were isolated according to previously published methods[57] with minor modifications. We stimulated cells with aldosterone (100 nmol l^{-1}) or vehicle (phosphate buffered saline) in the presence or absence of spironolactone (10 μmol l^{-1}) or apocynin (100 μmol l^{-1}), as indicated. Human MsrA cDNA was subcloned into pAd5-CMV-IRES-eGFP using blunt end ligation. Adenovirus was generated at the University of Iowa Gene Transfer Vector Core facility. The Rac1 dominant negative (N17rac1) construct[17], the CaMKII shRNA and rescue constructs[3] and the adenoviral CaMKII construct[58] are described elsewhere.

qRT-PCR. We isolated total RNA from ventricles using TRIzol reagent (Invitrogen) and from neonatal myocytes using an RNeasy Plus Mini kit (QIAGEN) according to the manufacturers' instructions. qRT-PCR for $Mmp9$ was performed with SYBR Green detection on an IQ Cycler (Bio-Rad) using the following primers: $Mmp9$ sense 5′–GAAGGCAAACCCTGTGTGTT–3′ and antisense 5′–AGAGTACTGCTTGCCCAGGA–3′ and $Gapdh$ sense 5′–CATTTCCTGGTATGACAATGAATACG–3′ and antisense 5′–TCCAGGGTTTCTTACTCCTTGGA–3′. We quantified mRNA levels using the ΔΔCt method. Specificity was determined using a melt curve analysis. Additional qRT-PCR was performed with the following TaqMan probes from ABI: $Ctgf$, Mm00515790_g1; $Col3a1$, Mm00802331_m1; $Col1a2$, Mm00483888_m1; and $Gapdh$ Mm99999915_g1.

Gelatin zymography. Tissue culture supernatant from treated primary cells was incubated with gelatin-sepharose (Amersham) in the presence of 1,10-phenanthroline (5 mmol l^{-1}) to inhibit metalloproteinase activity. Following binding and washing, the protein was released using a sample loading buffer. Samples were electrophoresed on Novex 10% zymogram gels co-polymerized with gelatin (Invitrogen). The SDS in the gel was exchanged for Triton in the washing buffer. The gel was allowed to develop overnight. The proteolytic activity was visualized as white bands on a background of Coomassie Brilliant Blue stain.

MsrA activity. We determined the relative reductase activity in whole-heart homogenates indirectly by spectrophotometric monitoring of the decline in the concentration of NADPH, which is consumed in the thioredoxin and thioredoxin reductase system during the recycling of MsrA[59].

MPO activity. We extracted MPO from whole hearts with hexadecyltrimethylammonium bromide–based lysis and assayed it according to previously published methods[24]. Briefly, the reaction of hydrogen peroxide and *o*-dianisidine dihydrochloride (reduced, colorless) was catalyzed by the addition of MPO in heart lysates to yield a yellow-orange end product that was detected spectrophotometrically at 460 nm. All readings were normalized to total protein.

Luciferase reporter assay. The mineralocorticoid- and glucocorticoid-responsive hormone response element firefly luciferase reporter was purchased from Clontech. The mouse $Mmp9$ promoter (−1,261 to +1) was subcloned into the pTAL-luc vector (Clontech) using blunt end ligation. The mutant $Mmp9$-promoter luciferase construct was obtained using a QuikChange Site Directed Mutagenesis kit (Stratagene). Transfection of a firefly luciferase reporter plus pRL-TK (Promega) was achieved with FuGENE 6 (Roche). We performed luciferase assays with the Dual Luciferase Reporter kit (Promega). Fluorescence was quantified on a microplate fluorometer.

Immunoblot and immunofluorescence. We performed immunoblotting and immunofluorescence as previously described[3] with minor modifications. DHE staining with light fixation was adapted from a published method[60] and then followed by immunofluorescence. Image processing for the relative intensity was performed using ImageJ. Staining and quantification were performed by investigators and technical personnel blinded to the treatments.

Statistics. The survival analysis was performed using a log-rank test. The contingency analysis was performed using a χ^2 test. All other statistical significance was determined using a Student's t test or one-way ANOVA, as appropriate. A Bonferroni's correction was applied for multiple comparisons. All values are expressed as means ± s.e.m. $P < 0.05$ was considered statistically significant.

Additional methods. Detailed methodology is described in the **Supplementary Methods**.

55. Weiss, R.M., Ohashi, M., Miller, J.D., Young, S.G. & Heistad, D.D. Calcific aortic valve stenosis in old hypercholesterolemic mice. *Circulation* **114**, 2065–2069 (2006).
56. Thiel, W.H. *et al.* Proarrhythmic defects in Timothy syndrome require calmodulin kinase II. *Circulation* **118**, 2225–2234 (2008).
57. Mohler, P.J. *et al.* Defining the cellular phenotype of "ankyrin-B syndrome" variants: human ANK2 variants associated with clinical phenotypes display a spectrum of activities in cardiomyocytes. *Circulation* **115**, 432–441 (2007).
58. Li, H. *et al.* Calmodulin kinase II is required for Ang II-mediated vascular smooth muscle hypertrophy. *Am. J. Physiol. Heart Circ. Physiol.* **298**, H688–H698 (2010).
59. Brot, N., Weissbach, L., Werth, J. & Weissbach, H. Enzymatic reduction of protein-bound methionine sulfoxide. *Proc. Natl. Acad. Sci. USA* **78**, 2155–2158 (1981).
60. Owusu-Ansah, E., Yavari, A. & Banerjee, U. A protocol for *in vivo* detection of reactive oxygen species. *Protocol Exchange* doi:10.1038/nprot.2008.23 (2008).